

Observational Astrophysics

12. Infrared astronomy

Rodolfo Smiljanic
Autumn/Winter 2021/2022

Nicolaus Copernicus Astronomical Center
Polish Academy of Sciences
ul. Bartycka 18
00-716 Warsaw, PL

E-mail: rsmiljanic@camk.edu.pl
Office: 115

<http://users.camk.edu.pl/rsmiljanic>

1 Introduction

Towards the red part of the spectrum, the human eye loses sensitivity at a wavelength of about 750 nm ($0.75\mu\text{m}$). One could then define the infrared (IR) to start there. This would include the *I* band, centered at about 806 nm (and indeed, the “I” stands for infrared). This region, however, is essentially still treated as an extension of visible astronomy, as the techniques and detectors are the same. At about $1.0\text{--}1.1\mu\text{m}$ the CCD detectors used in the visible are no longer useful and a different technology is needed. This change is one way used to mark the wavelength where IR astronomy begins. The convention is to divide the IR region into three parts (but note that the boundaries themselves are ill-defined):

1. Near-IR from $0.75\text{--}1.0\mu\text{m}$ to $5\mu\text{m}$;
2. Mid-IR from $5\mu\text{m}$ to $25\mu\text{m}$;
3. Far-IR from $25\mu\text{m}$ to $350\mu\text{m}$.

To make mid- and far-IR observations, one essentially needs to go above the atmosphere (although high altitudes and low water vapor help for observations in the M, N, and Q bands, and can open a few windows at 34 and $350\mu\text{m}$). At about $350\mu\text{m}$ (0.35 mm), radioastronomy-style receivers and techniques seem to be preferred. This wavelength marks the end of IR astronomy and the beginning of sub-mm astronomy (although some might consider this an extension of the far IR instead).

IR astronomy began with the detection of invisible solar rays by William Herschel (as discussed in a previous chapter of these notes). For the next steps in this history, have a look at Rieke (2009)¹ and Low et al. (2007)² and references therein. The real boost for IR astronomy came only in the 1960s, with the development of new detectors. This is when Harold L. Johnson³ extended the optical *UBVRI* system to the IR (Johnson 1966)⁴. Unfortunately, IR photometric systems proliferated in different observatories without the astronomers making a concerted effort to transform their IR

¹<https://ui.adsabs.harvard.edu/abs/2009ExA...25..125R/abstract>

²<https://ui.adsabs.harvard.edu/abs/2007ARA%26A...45..43L/abstract>

³See a biography here: <http://www.nasonline.org/publications/biographical-memoirs/memoir-pdfs/johnson-harold.pdf>

⁴<https://ui.adsabs.harvard.edu/abs/1966ARA%26A...4..193J/abstract>

photometry into a single standard system. This lack of standardization only changed in the 1980s with the work by Koornneef (1983a,b)⁵, Glass (1985)⁶, and Bessell & Brett (1988)⁷. It was only then that transformations between the different systems were well established and a homogenized system was put forward.

With these new developments, it became very clear that there were problems to transform magnitudes among the different systems and to reproduce previous observations. The precision of the magnitudes was not the one expected and, often, even data from the same observatory taken at different nights or a few hours apart were not consistent (Milone & Young 2011)⁸. This is the case because atmospheric extinction behaves differently from the case of visible wavelengths (see Young 1989; Young et al. 1994, for related discussions)⁹.

In parallel, airborne observations were being tried. These allowed detection of sources in the far IR, see Dolci & Dolci (1997)¹⁰ and Price (1988)¹¹ but also some discussion in Low et al. (2007) and Rieke (2009). The idea of flying IR missions to space also started to be explored in the 1960s (see Price 1988, 2009)¹². This culminated with the Infrared Astronomical Satellite (IRAS, see Neugebauer et al. 1984)¹³, which was the first IR space telescope to make an all-sky survey, at 12, 25, 60 and 100 μm .

Of course there is much more to this history. You can get a summary of more recent developments in the text recommended below.

2 Read this text

When discussing the observations in the optical, we temporarily skipped the discussion about detectors. We can not really do that in the case of IR observations. In addition to the extinction and emission from the atmosphere, thermal emission from the telescope and instrument, and the detector properties all become very important for IR observations.

For this topic, please read Tokunaga et al. (2013)¹⁴. This is a 76 pages summary of IR astronomy that covers the basics of everything, from the atmosphere to detectors and observing strategies for photometry and spectroscopy in the IR. It also summarizes information about several recent ground- and space-based surveys and facilities.

⁵See <https://ui.adsabs.harvard.edu/abs/1983A%26AS...51..489K/abstract> and <https://ui.adsabs.harvard.edu/abs/1983A%26A...128...84K/abstract>

⁶<https://ui.adsabs.harvard.edu/abs/1985IrAJ...17...1G/abstract>

⁷<https://ui.adsabs.harvard.edu/abs/1988PASP...100.1134B/abstract>

⁸https://link.springer.com/chapter/10.1007%2F978-1-4419-8050-2_6

⁹<https://ui.adsabs.harvard.edu/abs/1989LNP...341...6Y/abstract> and <https://ui.adsabs.harvard.edu/abs/1994A%26AS...105..259Y/abstract>

¹⁰https://www.sofia.usra.edu/sites/default/files/97-Whiting_AeroHistory.pdf

¹¹<https://ui.adsabs.harvard.edu/abs/1988PASP...100..171P/abstract>

¹²<https://ui.adsabs.harvard.edu/abs/2009SSRv...142..233P/abstract>

¹³For the paper see <https://ui.adsabs.harvard.edu/abs/1984ApJ...278L...1N/abstract>. If interested, you can find the data archive in <https://irsa.ipac.caltech.edu/Missions/iras.html>

¹⁴https://link.springer.com/referenceworkentry/10.1007%2F978-94-007-5618-2_3

3 Summary of concepts

- In the visible, Rayleigh and Mie scattering dominate the atmospheric extinction. These processes vary smoothly with wavelength and Bouguer’s (or Lambert’s law)¹⁵ can be used. In the IR, such a linear extinction law does not work anymore. The variations are strong and fast, as extinction is dominated by a series of individual atomic and molecular lines. The measurements are made over large bands, much wider than the width of single lines, where one could still hope to use a linear approximation. Moreover, molecular line absorption is usually saturated. Young (1989) discusses these issues in detail.
- The major absorption bands in the IR are caused by H₂O at 0.94, 1.13, 1.37, 1.87, 2.7, 3.2, 6.3, and > 16 μm ; by CO₂ at 2.0, 4.3, and 15 μm ; by N₂O at 4.5, and 17 μm ; by CH₄ at 3.3, and 7.7 μm ; and by O₃ at 9.6 μm . These gases are not necessarily uniformly mixed in the atmosphere, the proportions varying with height. The temperature structure of the atmosphere also varies with height. At some wavelengths within a given a band, the atmosphere may be completely opaque, while at others the transmission may be almost perfect. Computing the absorption from basic data in such cases is a complex endeavour.
- One big advantage of going to high altitudes or to space for IR observations is obviously to get above such absorption. Figure 1 compares the atmospheric absorption as seen from Mauna Kea with that seen by the Stratospheric Observatory for Infrared Astronomy (SOFIA, Young et al. 2012)¹⁶.
- In Fig. 2, a table shows the common designation of IR wavelength bands. Note, however, that there are numerous photometric filters designed to observe in these bands. Their passbands can vary even though they are usually called by the name of the band (i.e., one should not assume that the *K*-band filters in different observatories have the same properties, even though they are all designed to observe light in the IR *K* band).
- In the visible, one uses observations of standard stars to correct the observed magnitudes to a level above the atmosphere (i.e., correcting from the atmospheric extinction). In the IR, this is not possible. The extrapolation to “airmass zero” is non-linear. So in the IR one usually corrects the observations to an airmass of one. See Tokunaga & Vacca (2007) and references therein for a discussion.
- Airglow is a dominant source of background emission in the *J*, *H*, and most of the *K* bands. The emission lines are mostly from the hydroxyl radical OH¹⁷, formed at altitudes between 85-100 km (so high altitude observatories are still affected). The intensity can vary with observation direction and also with time (during the same night). See Fig. 3 for a model of the sky background at the Paranal observatory.

¹⁵The law states that the change in intensity of light travelling through a medium is proportional to the intensity and the path length, i.e. $dI_\nu = -e_\nu I_\nu ds$ where $-e_\nu$ is the extinction coefficient. Pierre Bouguer was a French scientist. See a biography in <https://mathshistory.st-andrews.ac.uk/Biographies/Bouguer/>. The law is discussed in Bouguer (1729), see https://archive.org/details/UFIE003101_T00324_PNI-2703_000000 for the original in French. Johann Heinrich Lambert was a Swiss-French scientist. See a biography in <https://mathshistory.st-andrews.ac.uk/Biographies/Lambert/>. The law is discussed in Lambert (1760), see https://archive.org/details/T00E039861_T00324_PNI-2733_000000 for the book in Latin.

¹⁶<https://ui.adsabs.harvard.edu/abs/2012ApJ...749L..17Y/abstract>

¹⁷By the so-called Meinel bands, first identified as belonging to OH by Aiden Meinel in Meinel (1950). See <https://physicstoday.scitation.org/doi/full/10.1063/PT.3.1568> for an obituary of Aiden Meinel.

- At about $2.3\mu\text{m}$, thermal emission from the telescope and atmosphere dominate over other sources of background radiation. Note that scattered light from the Moon becomes just a minor source of background.
- Zodiacal light (from dust in the solar system) is the dominant extra-terrestrial source of background. Up to about $3.5\mu\text{m}$ the zodiacal light background is from scattered sunlight. At longer wavelengths, the zodiacal light background is from dust emission. The background from sources outside the atmosphere is shown in Fig. 4.
- Typical night sky brightness in different bands are shown in the table of Fig. 5. Note the difference of about 10 magnitudes between the night sky brightness in the B and K bands.
- The background variability is perhaps the main difficulty when doing ground-based IR observations. The telescope and instrument temperatures are mostly constant. The sky emission, however, changes on very short time scales. Sky subtraction might be needed at a rate of several times per second. One should note that finding the optimal rate for sky background subtraction is dependent on the site characteristics, the sky conditions during the night, and the detector used.
- To deal with the night sky background, IR observations use the techniques of *chopping* and *nodding*. In chopping, the telescope secondary mirror alternates between two positions for on-source (or object plus sky) and off-source (or sky) observations. The on-source position, as the name implies, includes the target that is being observed. The off-source position is a reference sky position meant to observe only the sky background. Then one can isolate the source by subtracting the off-source “chop” from the on-source chop.
- Chopping is not enough though. Every minute or so, one still needs to slightly move the entire telescope to observe the same source from a shifted position. This is called nodding. In the second nodding, the chopping configuration is not changed but the sky area is on the other side of the source. This is needed to properly remove telescope background emission and eliminate any systematic trend or gradient in the background. See [this page](#) for an illustration of the chop and nod sequence and a better explanation than mine of these techniques.
- Chopping and nodding are usually needed for observations at wavelengths longer than about $3.5\mu\text{m}$. Nodding alone is still required for good background subtraction at shorter wavelengths than that.
- For infrared observations, the secondary mirror is made to be smaller than the beam reflected by the primary at its position. This is an arrangement that allows chopping to be done by moving the secondary. Note that in this case, the primary mirror no longer defines the entrance pupil of the system, which is now defined by the secondary mirror.
- Bolometers¹⁸ are the most common example of thermal detector used in IR astronomy. Thermal detectors rely on changes in the electrical or mechanical properties (e.g., resistance,

¹⁸Samuel Pierpont Langley, American astronomer and aviator, invented the first bolometer in 1880, see Langley (1880) in <https://doi.org/10.2307/25138616>. For a biography see https://link.springer.com/referenceworkentry/10.1007/978-0-387-30400-7_821 and also Barr (1963) in <https://ui.adsabs.harvard.edu/abs/1963InfPh...3..195B/abstract>. However, astronomical interest in the bolometer only increased with the invention of the liquid helium cooled gallium-doped germanium bolometer in 1961 by the American physicist Frank Low, see Low (1961) in <https://ui.adsabs.harvard.edu/abs/1961JOSA...51.1300L/abstract>. For a biography see Rieke (2014) in <http://www.nasonline.org/publications/biographical-memoirs/memoir-pdfs/low-frank.pdf>.

voltage, volume) of a sensing material caused by the heating from the incident radiation. The sensitivity of bolometers is wavelength independent and the temperature difference is proportional to the intensity of the radiation. In practice, the wavelength range of the incident radiation can be limited by a filter. In general, thermal detectors are slow as they require time to heat up after the incident flux has been absorbed.

- Another type of detector used in IR astronomy are photon detectors of the photoconductor type which are made of semiconductors¹⁹. An electrical output signal is detected when incident photons have energy enough to free electrons inside the semiconductor crystal. In other words, the electrons are promoted from the valence energy band across the *intrinsic* band gap to the conduction energy band. The smaller the band gap, the longest the wavelength that can be detected. In addition, the smaller the band gap, the easiest it is for thermally excited electrons to just enter the conduction band unwanted. Therefore, such detectors must be cooled to low temperatures, to minimize the signal from thermally excited electrons. For the near IR, liquid nitrogen (77 K) is used to cool down the detectors. In the mid IR, liquid helium (4 K) is used. In the far IR, temperatures down to 100 mK are used.
- Photon detectors can alternatively use extrinsic photoconductivity from impurities (i.e. also called dopants, which are added to the semiconductor material). In this case, the photon frees an electron from an impurity atom, creating an electron-hole pair. A current is created when either the hole or the electron move through the material in response to an electric field. Because it takes less energy to free an electron from an impurity atom, extrinsic photon detectors can operate at longer wavelengths (i.e. the band gap is reduced).
- Two materials used for intrinsic photoconductor detectors are indium antimonide (InSb), with a cutoff wavelength at about 5 μm , and mercury cadmium telluride (HgCdTe). The latter has a band gap that can be adjusted by varying the fraction of cadmium. The cutoff wavelength can be changed between $\sim 1\text{--}20$ μm . Silicon and germanium with the addition of dopants are used as extrinsic photoconductor detectors.
- The amount of impurities cannot be increased arbitrarily, otherwise one forms an impurity band and increases the dark current. It was discovered that applying mechanical stress to the detector material increases its response to long wavelengths. Stressed photoconductor detectors of Ga-doped Ge (Ge:Ga) can be sensitive to wavelengths up to 200 μm .
- Another variation of the photoconductor detector are the so-called impurity band conduction (IBC) or blocked impurity band (BIB) detectors. In these, the doping level is high enough to produce an impurity band. The large dark current is blocked with the introduction of an undoped blocking layer.
- The dark current mentioned above is the signal that appears from spurious conduction electrons that are not created by the arriving photons. Sources of dark include thermal excitation and electrical leakage within the detector. In the visible, modern detectors nowadays have negligible dark currents. For most near-IR arrays, the counts created by the dark current are at a level much below the signal from background sources. Thus, usually, the step of correcting the data from the dark current can be skipped.

¹⁹See Wikipedia <https://en.wikipedia.org/wiki/Semiconductor> and Section 5.5.2 of McLean (2008) in <https://link.springer.com/book/10.1007%2F978-3-540-76583-7>.

- Creating detector arrays (i.e., two-dimensional multi-pixel detectors as opposed to single-cell detectors) for use in IR has been a big technological challenge. Several problems with the readout modes (IR arrays are not charge transfer devices; each pixel is readout independently), poor quantum efficiency, temperature of operation, properties of the materials, filling factors (limitations to closely pack the pixels without dead regions in-between them) etc, had to be overcome. For a review of these developments, see Rieke (2007).
- The detector quantum efficiency is defined as the fraction of the incident photons that produce conduction electrons in the detector. A comparison between the quantum efficiency of different types of detectors across a range in wavelengths is shown in Fig. 6.
- Semiconductor materials can also be used to produce a different type of detector, the photodiodes. They are a junction of n-type and p-type materials²⁰. The formation of a p-n junction creates, between the two materials, a region depleted of charges and also a potential barrier that restrains the flow of electrons from the n-type material. When light is absorbed near the junction, an electron-hole pair is created. The potential difference across the junction draws the electrons towards the region of positive potential, before the recombination can occur. This creates a current generated by the illuminating radiation, which can be monitored and used to measure the intensity of the light.
- We will look in more detail at the signal-to-noise equations and cases later. For now, you should keep in mind that for ground-based mid- and far-IR photon detectors, when doing imaging or low-resolution spectroscopy, one usually works at the background-limited regime (where the signal from the background \gg signal of the source) and in this case the signal-to-noise ratio (SNR) increases linearly with the source flux (while in the optical, where the source signal \gg the background signal, the SNR increases with the square root of the source flux).
- IR-optimized telescopes are designed to minimize the surfaces contributing with thermal background. The supporting structures of the secondary are hidden behind the mirror itself. Light baffles (that block stray light from random directions) are removed. A hole can be made in the center of the secondary to avoid reflection of thermal radiation coming from the Cassegrain focus. Low-emissivity coatings are used (such as gold or a type of overcoated silver). Instruments are built with a cold stop at the pupil that blocks thermal radiation not coming from the secondary mirror.
- In the IR, the seeing is better than in the visible. In addition, the isoplanatic angle is also larger, so the region where to look for natural guide stars for adaptive optics is increased. However, many IR observations are done in regions highly obscured by dust, where finding bright sources is usually not possible.
- IR instruments are cooled down to reduce thermal background. Materials have to be carefully chosen to work in such temperatures. Note that the dimensions will change during the cool-down process. Different materials can shrink by distinct amounts, and that can cause problems. All this has to be properly taken into account in the design. Each component of the instrument has to be designed and built in a way that the correct dimensions are

²⁰n-type is a semiconductor doped with impurity atoms that have more valence electrons than the semiconductor. They thus donate the extra negative charges to the conduction band. p-type, on the other hand, are doped with impurity atoms that have less valence electrons than the semiconductor. The impurity adds a hole to the valence band, ready to accept any available electron.

obtained after the instrument is cooled down. Cooling down the telescope itself is usually not an option, as this would create condensation.

- As mentioned above, important differences of imaging in the IR compared to the optical are the high-level and the variability of the background. While in the optical one can integrate the signal from the source for long times, in the IR each individual observation is short.
- Another issue are defects on the detector array (i.e., bad pixels or regions of low quantum efficiency). To correct for these effects, one can use dithering. This is a technique of taking repeated images of the source with the telescope slightly moved by a few arcseconds, so that the source falls in different regions of the detector. Like this, it can be avoided that bad detector regions affect the source in every image. Defects can then be masked out during the reduction process.
- For standard stars to be used in IR photometry, see the references given in Section 7.1 of Tokunaga et al. (2013). Note that Vega itself has an IR excess emission beyond about $12\mu\text{m}$ Aumann et al. (1984)²¹ caused by a debris disk around the star (Su et al. 2005)²².
- Sirius has been suggested by many authors as a good alternative to Vega. It is an A0-A1 star, rotating slowly, and without IR excess. See Rieke et al. (2021)²³ for a report on work to establish Sirius as primary standard and tie other stars to it as secondary standards, in preparation for JWST observations.
- High-resolution spectroscopy in the IR works more or less in the same way as in the optical. In this case, longer exposures are possible. In high-resolution, the individual lines of the background emission are resolved, and the regions in between have lower background. One needs to avoid saturating the OH lines and also entering into the nonlinearity regime of the detectors. The background OH lines can even help with the wavelength calibration of the spectra. If the slit is long enough, nodding the object along the slit is used to help in the subtraction of the thermal background from the sky and telescope (and also to help removing the dark current, if needed). The slit has to be long, so the PSFs of the two observations do not overlap. If the slit is not long enough, one nod is done in a sky position instead.
- Spectral lines from the atmosphere can be corrected from the spectra with the observation of “telluric standards”, as long as the lines are not saturated. Telluric standards are stars whose spectra are featureless in the same region, so that the lines that appear are only the telluric ones (the ones from Earth’s atmosphere). Alternatively, theoretical atmospheric spectra can also be computed and used for the correction. Molecfit (Smette et al. 2015)²⁴ is one of such tools, developed for use with ESO VLT data but general enough to be used for other instruments and telescopes as well.
- All parts of the spectrograph still need to be cooled to low temperatures, to prevent that thermal photons from all the structures (slit, grating, walls) reach the detector.

²¹<https://ui.adsabs.harvard.edu/abs/1984ApJ...278L..23A/abstract>

²²<https://ui.adsabs.harvard.edu/abs/2005ApJ...628..487S/abstract>

²³<https://arxiv.org/abs/2111.10444>

²⁴<https://ui.adsabs.harvard.edu/abs/2015A%26A...576A..77S/abstract>

4 Additional reading

For a history of the development of IR detectors, see Rogalski (2012)²⁵. For a review of IR arrays used in astronomy, see Rieke (2007)²⁶. An extensive discussion of IR array detectors and electronic imaging in the IR is given in Chapter 11 of McLean (2008)²⁷.

For an informative, although old, text on IR, see the “Handbook of Infrared Astronomy” (Glass 1999). This text covers topics like the sky, detectors and instruments, science, techniques, etc.

For recommendations on a infrared passband system designed to minimize the dependence of the photometry on water vapor bands see Milone & Young (2005)²⁸ and Milone & Young (2007)²⁹. For discussions about the absolute photometric calibration in the IR see Price (2004)³⁰, Rieke et al. (2008)³¹, and Engelke et al. (2010)³².

To read more about far-IR facilities and plans for the future, see Farrah et al. (2019)³³.

For a discussion of the spectral data reduction procedures, see Cushing et al. (2004)³⁴.

References

- Aumann, H. H., Gillett, F. C., Beichman, C. A., et al. 1984, ApJL, 278, L23
- Barr, E. S. 1963, Infrared Physics, 3, 195,IN1,197,IN3,201
- Bessell, M. S. & Brett, J. M. 1988, PASP, 100, 1134
- Bouguer, P. 1729, Essai d’optique sur la gradation de la lumière (Claude Jombert)
- Cushing, M. C., Vacca, W. D., & Rayner, J. T. 2004, PASP, 116, 362
- Dolci, W. & Dolci, W. 1997, in 1997 World Aviation Congress, 5609
- Engelke, C. W., Price, S. D., & Kraemer, K. E. 2010, AJ, 140, 1919
- Farrah, D., Smith, K. E., Ardila, D., et al. 2019, Journal of Astronomical Telescopes, Instruments, and Systems, 5, 020901
- Glass, I. S. 1985, Irish Astronomical Journal, 17, 1
- Glass, I. S. 1999, Handbook of Infrared Astronomy (Cambridge University Press)

²⁵<https://ui.adsabs.harvard.edu/abs/2012OERv...20..279R/abstract>

²⁶<https://ui.adsabs.harvard.edu/abs/2007ARA%26A...45...77R/abstract>

²⁷<https://link.springer.com/book/10.1007%2F978-3-540-76583-7>

²⁸<https://ui.adsabs.harvard.edu/abs/2005PASP...117..485M/abstract>

²⁹<https://ui.adsabs.harvard.edu/abs/2007ASPC...364..387M/abstract>

³⁰<https://ui.adsabs.harvard.edu/abs/2004SSRv...113..409P/abstract>

³¹<https://ui.adsabs.harvard.edu/abs/2008AJ...135.2245R/abstract>

³²<https://ui.adsabs.harvard.edu/abs/2010AJ...140.1919E/abstract>

³³<https://ui.adsabs.harvard.edu/abs/2019JATIS...5b0901F/abstract>

³⁴<https://ui.adsabs.harvard.edu/abs/2004PASP...116..362C/abstract>

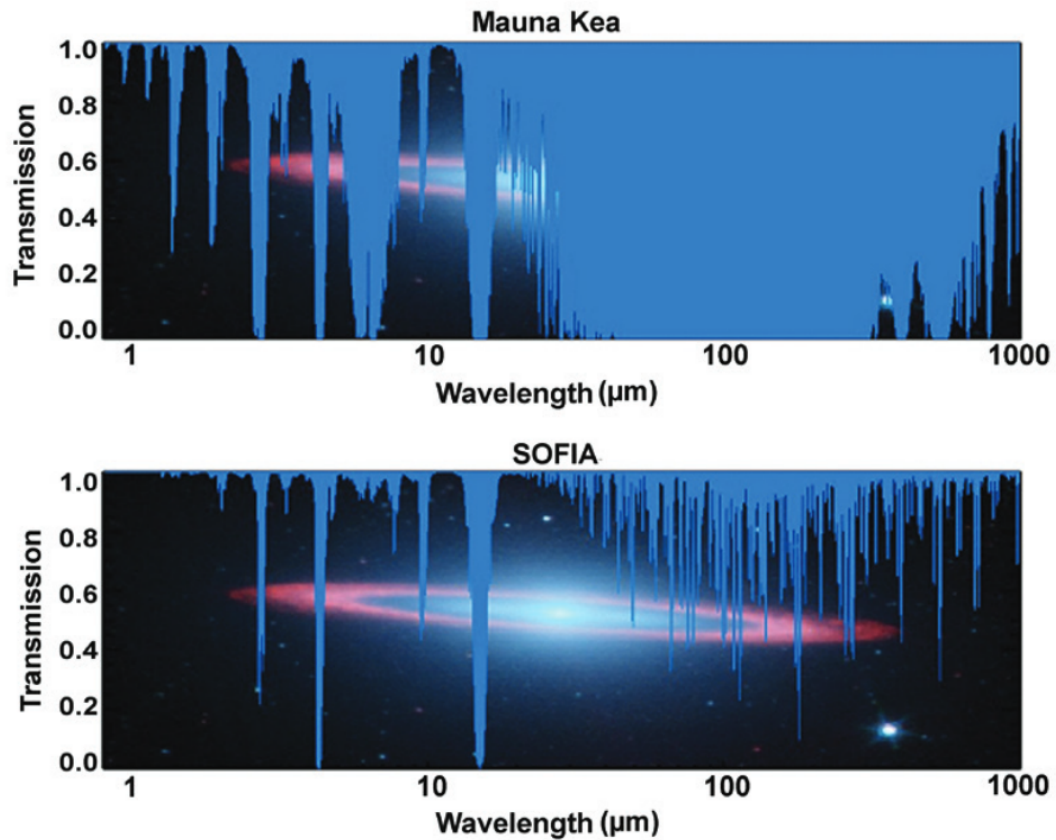


Figure 2. Typical atmospheric transparency at an altitude of 45,000 feet as compared with the transparency at the summit of Mauna Kea, an altitude of 13,800 ft. Blue strips extending all the way from the top to bottom of the panels indicate wavelengths of light blocked by Earth's atmosphere. The difference between the lower and upper panels is striking: at SOFIA's operating altitude, the atmosphere above the observatory is nearly transparent across this entire wavelength range, with the exception of two narrow blocked bands. **SOFIA enables observations that are impossible even from observatories on high mountain peaks.** Background: False-color infrared image of the Sombrero Galaxy (NASA/JPL-Caltech/Spitzer).

Figure 1: Atmospheric absorption from Mauna Kea and with SOFIA. Credit: https://www.sofia.usra.edu/sites/default/files/Other/Documents/science_case-final.pdf

TABLE I Common Infrared Photometric Bands

Band designation	Wavelength range
J	1.1–1.4
H	1.5–1.8
K	2.0–2.4
L	3.5–4.5
M	4.4–5.0
N	8.0–12.6
Q	16.5–23.0

Figure 2: Designation and wavelength range of the common infrared bands. See also Fig. 3.7 of the Tokunaga et al. (2013) text recommended above. Credit: Table 1 from Thompson (2003), see <https://www.sciencedirect.com/science/article/pii/B0122274105003380>.

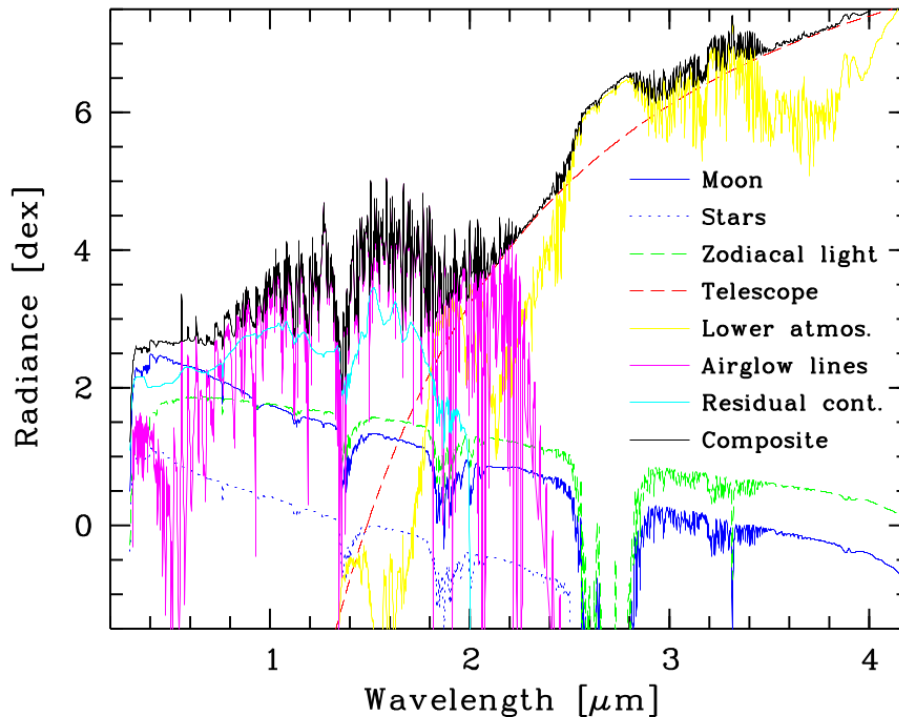


Figure 3: Sky model of the background at Paranal. Credit: The Cerro Paranal Advanced Sky Model, see <https://www.eso.org/sci/software/pipelines/skytools/skymodel>

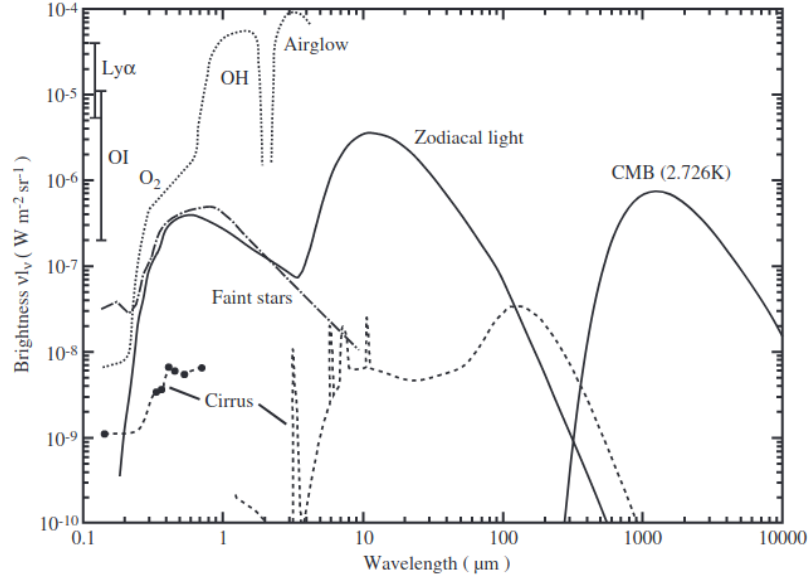


Figure 4: Sky brightness in the upper atmosphere. Credit: Figure 1 from Leinert et al. (1998), see <https://ui.adsabs.harvard.edu/abs/1998A%26AS..127....1L/abstract>.

Table 6: Typical sky model and literature night-sky brightnesses in mag arcsec⁻² for zenith, New Moon, faint zodiacal light, and different 10.7 cm solar radio fluxes $S_{10.7}$ in sfu.

Source	Site	$S_{10.7}$	U	B	V	R	I	J	H	K
Benn & Ellison [2007]	La Palma	80	22.0	22.7	21.9	21.0	20.0	16.6	14.4	12.0
Walker [1987]	Cerro Tololo	90	22.0	22.7	21.8	20.9	19.9			
Krisciunas et al. [2007]	Cerro Tololo	130	22.1	22.8	21.8	21.2	19.9			
Mattila et al. [1996]	La Silla	150		22.8	21.7	20.8	19.5			
Patat [2008]	Cerro Paranal	160	22.4	22.7	21.7	20.9	19.7			
Cuby et al. [2000]	Cerro Paranal	170						16.5	14.4	13.0
Patat [2003]	Cerro Paranal	180	22.3	22.6	21.6	20.9	19.7			
Sky model	Cerro Paranal	90	22.3	22.9	22.0	21.2	19.8	16.8	14.4	12.8
		130	22.1	22.8	21.8	21.0	19.7	16.7	14.4	12.8
		180	21.9	22.6	21.6	20.9	19.6	16.5	14.4	12.8

Figure 5: Night sky brightness in different bands. Credit: The Cerro Paranal Advanced Sky Model, see <https://www.eso.org/sci/software/pipelines/skytools/skymodel>

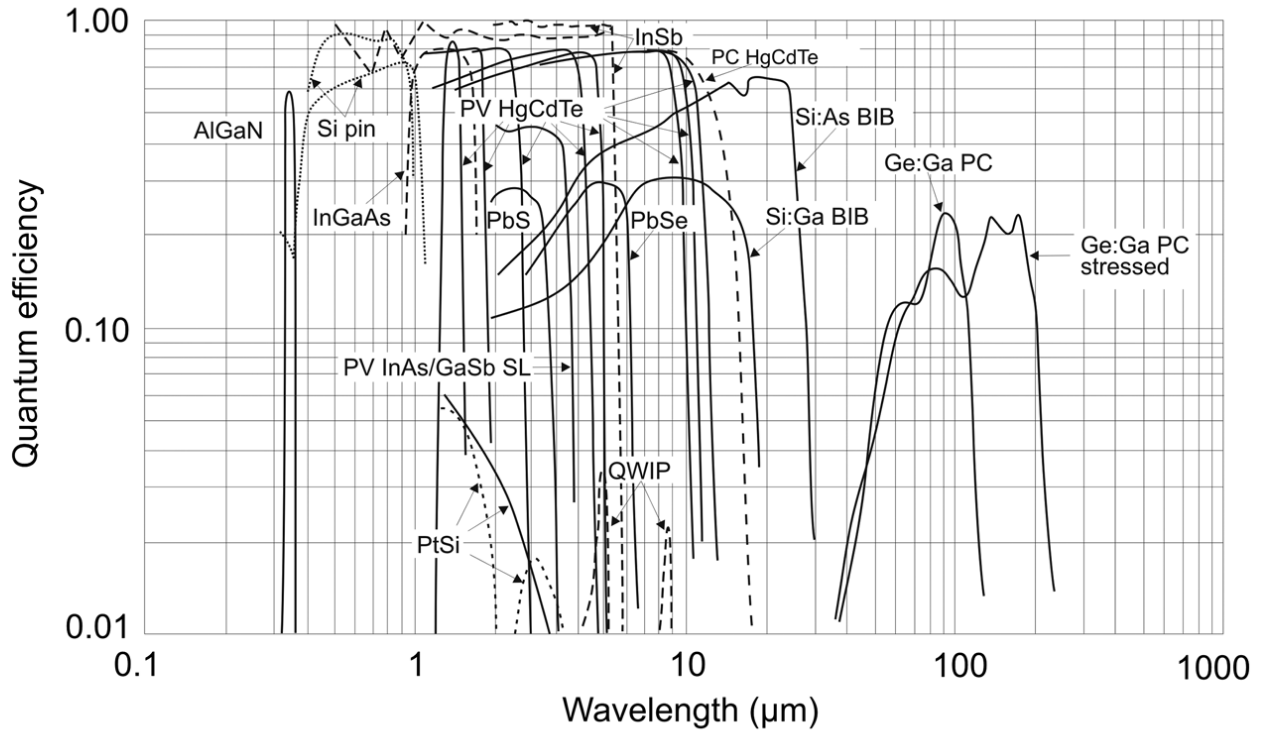


Figure 6: Quantum efficiency of different detectors. Credit: Figure 1.9 in Chapter 1 of Rogalski et al. (2018), see <https://spie.org/samples/PM280.pdf>.

Johnson, H. L. 1966, *ARA&A*, 4, 193

Koornneef, J. 1983a, *Astronomy and Astrophysics Supplement*, 51, 489

Koornneef, J. 1983b, *A&A*, 500, 247

Lambert, J. H. 1760, *Photometria sive de mensura et gradibus luminis, colorum et umbrae* (sumptibus viduae E. Klett, typis CP Detleffsen)

Langley, S. P. 1880, in *Proceedings of the American Academy of Arts and Sciences*, Vol. 16, JSTOR, 342–358

Leinert, C., Bowyer, S., Haikala, L. K., et al. 1998, *Astronomy and Astrophysics Supplement*, 127, 1

Low, F. J. 1961, *Journal of the Optical Society of America* (1917-1983), 51, 1300

Low, F. J., Rieke, G. H., & Gehrz, R. D. 2007, *ARA&A*, 45, 43

McLean, I. S. 2008, *Electronic Imaging in Astronomy*

Meinel, I. A. B. 1950, *ApJ*, 111, 555

Milone, E. F. & Young, A. T. 2005, *PASP*, 117, 485

- Milone, E. F. & Young, A. T. 2007, in *Astronomical Society of the Pacific Conference Series*, Vol. 364, *The Future of Photometric, Spectrophotometric and Polarimetric Standardization*, ed. C. Sterken, 387
- Milone, E. F. & Young, A. T. 2011, in *Astrophysics and Space Science Library*, Vol. 373, *Astronomical Photometry: Past, Present, and Future*, ed. E. F. F. Milone & C. Sterken, 127
- Neugebauer, G., Habing, H. J., van Duinen, R., et al. 1984, *ApJL*, 278, L1
- Price, S. D. 1988, *PASP*, 100, 171
- Price, S. D. 2004, *Space Science Reviews*, 113, 409
- Price, S. D. 2009, *Space Science Reviews*, 142, 233
- Rieke, G. H. 2007, *ARA&A*, 45, 77
- Rieke, G. H. 2009, *Experimental Astronomy*, 25, 125
- Rieke, G. H. 2014, *Biographical Memoirs of the National Academy of Sciences*
- Rieke, G. H., Blaylock, M., Decin, L., et al. 2008, *AJ*, 135, 2245
- Rieke, G. H., Su, K. Y. L., Sloan, G. C., & Schlawin, E. 2021, arXiv e-prints, arXiv:2111.10444
- Rogalski, A. 2012, *Opto-Electronics Review*, 20, 279
- Rogalski, A. W., Kopytko, M. E., & Martyniuk, P. M. 2018, *Antimonide-based infrared detectors: a new perspective (SPIE-The International Society for Optics and Photonics)*
- Smette, A., Sana, H., Noll, S., et al. 2015, *A&A*, 576, A77
- Su, K. Y. L., Rieke, G. H., Misselt, K. A., et al. 2005, *ApJ*, 628, 487
- Thompson, R. I. 2003, in *Encyclopedia of Physical Science and Technology*, 3rd edn., ed. R. A. Meyers (New York: Academic Press), 771–791
- Tokunaga, A. T. & Vacca, W. D. 2007, in *Astronomical Society of the Pacific Conference Series*, Vol. 364, *The Future of Photometric, Spectrophotometric and Polarimetric Standardization*, ed. C. Sterken, 409
- Tokunaga, A. T., Vacca, W. D., & Young, E. T. 2013, *Infrared Astronomy Fundamentals*, ed. T. D. Oswalt & H. E. Bond, 99
- Young, A. T. 1989, *Extinction and Transformation*, ed. E. F. Milone, Vol. 341, 6
- Young, A. T., Milone, E. F., & Stagg, C. R. 1994, *Astronomy and Astrophysics Supplement*, 105, 259
- Young, E. T., Becklin, E. E., Marcum, P. M., et al. 2012, *ApJL*, 749, L17